2007 IEEE International Conference on
Robotics and Automation
Roma, Italy, 10-14 April 2007

Adaptive Control of Manipulators via an Extension to the Error-Based Minimal Control Synthesis with Integral Action Algorithm

K. Koganezawa and D. P. Stoten

Abstract—**This paper introduces an extension to the original error-based minimal control synthesis with integral action (Er-MCSI) algorithm, for controlling serial link manipulators. Minimal control synthesis (MCS) methods have a number of attractive features: no *a priori* knowledge of the robot structure is required; eg. no need for parameter identification, no precise adjustment of control parameters is necessary and proven stability. After a brief summary of the basic MCS algorithm, we introduce the new algorithm, which provides a more robust environment in terms of gain wind-up protection. A proof of stability is also provided, together with simulation studies upon serial link manipulators, which demonstrate the excellent performance of the proposed algorithm, even under severe test conditions.**

I. Introduction

Over the last two decades there has been considerable effort expended on introducing adaptive schemes for controlling mechanical manipulators [1]-[9]. The prime motivation for introducing such schemes is that the manipulator is usually a non-linear, multi-input, multi-output (MIMO) system, which has dynamically coupled degrees of freedom (DOF), together with significant parameter uncertainty. In such circumstances the widely-used PID controller, for example, requires a redesign on each occasion that the manipulator payload or operating point changes.

All of the methods cited in the references [1]-[9] require on-line identification of some unknown physical parameters of the manipulator. This implies that, although on-line identification schemes make it unnecessary to know values of the parameters in advance, it does require that the manipulator dynamics have to be precisely described as a known set of non-linear dynamic equations. Moreover, persistently exciting conditions on the demand signals are mandatory for guaranteed convergence of the estimated parameters [3], [6]. In addition, estimated parameters will be noise-sensitive, because their update laws are based on the use of first and second derivatives of the link displacements. These issues have hampered the practical use of adaptive control schemes for manipulator control, using the approaches taken by [1]-[9].

In parallel with the above research effort, an adaptive control scheme based on the *minimal control synthesis* (MCS) algorithm has been applied within a number of engineering fields: for example, the control of AC motors [10], the control of permanent magnet synchronous motors [11], the control of vehicle dynamics [12] and satellite attitude control [13]. The MCS algorithm [14]-[17] extended model-reference adaptive control (MRAC) [18] and significantly simplified the controller design. In particular, MCS requires no *a priori* information on the plant model or on the controller gains, which is in sharp contradistinction with the standard MRAC formulation. In addition, MCS does not require any on-line system identification procedure.

The adaptive control scheme employed in this study is based upon the *error-based minimal control synthesis with integral action* (Er-MCSI) algorithm, [19], which removes the operating-point sensitivity that is a feature of the original MCS/MRAC algorithms. Thus, adaptive parameters can be set without reference to plant operating regimes.

This paper is organized as follows. Section II provides a brief introduction to the standard MCS and also the Er-MCSI algorithms. In the section III we propose a generalized improvement to the Er-MCSI algorithm, with an associated stability proof based upon passivity theory. Section IV is devoted to simulation studies on a serial link manipulator and relevant conclusions are drawn in section V.

II. The MCS and Er-MCSI Algorithms

This section briefly describes the historical development of the MRAC, the MCS and the Er-MCSI algorithms. Analytic details are described in the following section.

Fig.1 shows the block diagram of the adaptive feedback control system based on the MCS algorithm. The adaptive feedforward gain, $\boldsymbol{K}_r(t)$, and feedback gain, $\boldsymbol{K}(t)$, are generated via:

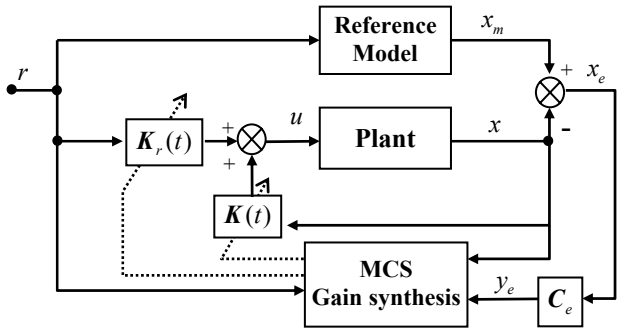

Fig.1 Block diagram of the MCS adaptive control

Manuscript received September 15, 2006.
K Koganezawa is with the Department of Mechanical Engineering, Tokai University, Kanagawa 259-1292, JAPAN;(kogane@keyaki.cc.u-tokai.ac.jp)
D P Stoten is with the Department of Mechanical Engineering, University of Bristol, Bristol BS81TR, UK; (d.p.stoten@bristol.ac.uk)

$$\boldsymbol{K}_r(t) = \alpha\int_0^t \boldsymbol{y}_e(\tau)\boldsymbol{r}^T(\tau)d\tau + \beta\boldsymbol{y}_e(\tau)\boldsymbol{r}^T(\tau),$$
$$\boldsymbol{K}(t) = \alpha\int_0^t \boldsymbol{y}_e(\tau)\boldsymbol{x}^T(\tau)d\tau + \beta\boldsymbol{y}_e(\tau)\boldsymbol{x}^T(\tau) \quad (1)$$

which require the provision of just two scalar weighting parameters, α and β. The control signal, $\boldsymbol{u}(t)$, is then generated by:

$$\boldsymbol{u}(t) = \boldsymbol{K}(t)\boldsymbol{x}(t) + \boldsymbol{K}_r(t)\boldsymbol{r}(t) \quad (2)$$

The essential difference between the MCS algorithm and MRAC is that, in the latter, an *a priori* knowledge of the plant dynamics is required to generate fixed gains, $\boldsymbol{K}$ and $\boldsymbol{K}_r$, and the adaptive terms are then considered to be merely 'small' quantities. Hence the corresponding MRAC control signal is:

$$\boldsymbol{u}(t) = -[\boldsymbol{K} - \delta\boldsymbol{K}(t)]\boldsymbol{x}(t) + [\boldsymbol{K}_r + \delta\boldsymbol{K}_r(t)]\boldsymbol{r}(t) \quad (3)$$

In addition, within the MCS stability proof there is no requirement for a knowledge of the plant dynamics, in contradistinction to the more conventional MRAC algorithm.

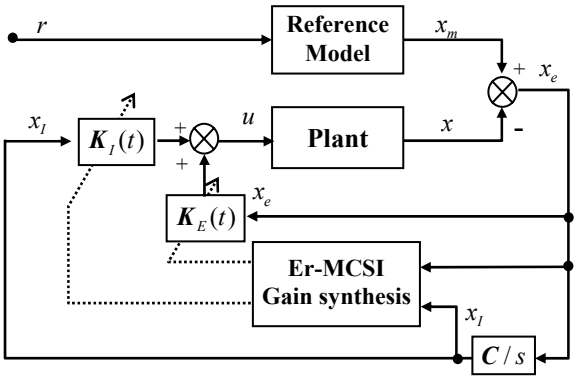

Fig.2 Block diagram of the Er-MCSI adaptive control

The error based minimum control synthesis with integral action (Er-MCSI) algorithm [19] is a modification of MCS. As indicated in Fig.2, the adaptive gains $\boldsymbol{K}_I(t)$ and $\boldsymbol{K}_E(t)$ are generated from the state error vector only. The control signal is therefore generated as follows:

$$\boldsymbol{u}(t) = \boldsymbol{K}_I(t)\boldsymbol{x}_I(t) + \boldsymbol{K}_E(t)\boldsymbol{x}_E(t) \quad (4)$$

where $\boldsymbol{x}_I(t)$ is the integral of error and the gains themselves are generated by equations of the same structure as (1).

This means that the adaptive gains and the control signal are insensitive to the operating points of both the plant and the reference model, so that the adaptive weighting parameters, α and β, can be specified irrespective of these operating points. Correspondingly, relatively high gains and faster adaptation can be achieved.

III. The Generalized Er-MCSI Algorithm

This study focuses on the Er-MCSI scheme but proposes a new, generalized, version of the algorithm, which is now formulated in this section.

A. Plant system

We assume that the MIMO plant that has m-DOF, each of which is described by the n^{th}-order non-linear differential equation:

$$\dot{\boldsymbol{x}} = \boldsymbol{A}(t)\boldsymbol{x} + \boldsymbol{B}_E\boldsymbol{B}(t)\boldsymbol{u}(t) + \boldsymbol{d}(t) \quad (5)$$

where:

$$\boldsymbol{x} = \begin{bmatrix} x_1 & \dot{x}_1 & \cdots & x_1^{(n-1)} & \cdots & \cdots & x_m & \dot{x}_m & \cdots & x_m^{(n-1)} \end{bmatrix}^T \in \Re^{mn}$$

is a state space vector and

$$\boldsymbol{A}(t) = diag\{\boldsymbol{A}_1(t),\ \cdots,\ \boldsymbol{A}_m(t)\} \quad \in \Re^{mn\times mn}$$

has block matrices in the canonical form:

$$\boldsymbol{A}_i(t) = \begin{bmatrix} 0 & 1 & 0 & \cdots & 0 \\ \vdots & \ddots & \ddots & \ddots & \vdots \\ \vdots & & \ddots & \ddots & 0 \\ 0 & & \cdots & 0 & 1 \\ -a_{i1}(t) & -a_{i2}(t) & \cdots & \cdots & -a_{in}(t) \end{bmatrix} \in \Re^{n\times n}\ (i = 1,\cdots,m)$$

$\boldsymbol{B}(t)$ is an $m\times m$ strictly positive definite symmetric matrix (often it will be the inverse mass/inertia matrix in a robotic system). Also:

$$\boldsymbol{B}_E = diag\{\underbrace{\boldsymbol{b}_0, \boldsymbol{b}_0, \cdots \boldsymbol{b}_0}_{(m)}\} \in \Re^{mn\times m}, \text{ with } \boldsymbol{b}_0 = \begin{bmatrix} 0 \cdots 0 & 1 \end{bmatrix}^T \in \Re^n$$

$\boldsymbol{u}(t) = \begin{bmatrix} u_1(t) & u_2(t) & \cdots & u_m(t) \end{bmatrix}^T \in \Re^m$ is an input vector, and $\boldsymbol{d}(t) = diag\{\boldsymbol{d}_1, \boldsymbol{d}_2, \cdots, \boldsymbol{d}_m\} \in \Re^{mn\times m}$, with $\boldsymbol{d}_i = [0 \cdots 0\ d_i]^T \in \Re^n$ is a vector that includes any non-linear terms (eg. Coriolis terms, centrifugal terms and gravitational terms). Hence, the plant is a coupled, non-linear, dynamical system. It is assumed that the non-linear terms are bounded in their values across the entire state-space.

B. Reference model system

We introduce a linear reference model as follows:

$$\dot{\bar{\boldsymbol{x}}}(t) = \bar{\boldsymbol{A}}\bar{\boldsymbol{x}}(t) + \bar{\boldsymbol{B}}\boldsymbol{r}(t) \quad (6)$$

where:

$$\bar{\boldsymbol{x}}(t) = \begin{bmatrix} \bar{x}_1(t)\ \dot{\bar{x}}_1(t) \cdots \bar{x}_1^{(n-1)}(t) \cdots & \cdots \bar{x}_m(t)\ \dot{\bar{x}}_m(t) \cdots \bar{x}_m^{(n-1)}(t) \end{bmatrix}^T \in \Re^{mn}$$

is a model state space vector, and:

$$\bar{\boldsymbol{A}} = diag\{\bar{\boldsymbol{A}}_1, \bar{\boldsymbol{A}}_2, \cdots, \bar{\boldsymbol{A}}_m\} \in \Re^{mn\times mn}$$

with $\bar{\boldsymbol{A}}_i = \begin{bmatrix} 0 & 1 & 0 & \cdots & 0 \\ \vdots & \ddots & \ddots & \ddots & \vdots \\ \vdots & & \ddots & \ddots & 0 \\ 0 & & \cdots & 0 & 1 \\ -\bar{a}_{i1} & -\bar{a}_{i2} & \cdots & \cdots & -\bar{a}_{in} \end{bmatrix} \in \Re^{n\times n}$

$$\bar{\boldsymbol{B}} = diag\{\bar{\boldsymbol{b}}_1, \bar{\boldsymbol{b}}_2, \cdots, \bar{\boldsymbol{b}}_m\} \in \Re^{mn\times m}, \text{ with } \bar{\boldsymbol{b}}_i = \begin{bmatrix} 0 \cdots 0\ \bar{b}_i \end{bmatrix}^T \in \Re^n$$

and $\boldsymbol{r}(t) = \begin{bmatrix} r_1(t)\ r_2(t) \cdots r_m(t) \end{bmatrix}^T$ is the reference input vector.

In the reference model, the dynamics of the multiple DOF are completely decoupled and each DOF has a stable transfer function $(s\boldsymbol{I} - \bar{\boldsymbol{A}}_i)^{-1}\bar{\boldsymbol{b}}_i\ \ (i = 1,\cdots,m)$.

C. State error dynamics

We introduce two vectors related to the model following error:

The proportional state error vector: $\boldsymbol{x}_{PE}(t) = \bar{\boldsymbol{x}}(t) - \boldsymbol{x}(t)$ (7)

The filtered state error vector: $\boldsymbol{x}_{FE}(t) = \int_0^t e^{\varepsilon_0(\tau-t)}\boldsymbol{x}_{PE}(\tau)d\tau$ (8)

where ε_0 is a sufficiently small value so that $\boldsymbol{x}_{FE}(t)$ has virtually the dynamic properties of an integrated signal, but with a finite low frequency gain of $1/\varepsilon_0$. In previous work, standard Er-MCSI has used the purely integrated vector of $\boldsymbol{x}_{PE}(t)$, which has occasionally caused the wind-up of the adaptive gains [19]. Thus, the reason for adding the new filtering effect is to cope with this wind-up phenomenon of adaptive gains, due to input saturation and signal noise, [20], and thus to stabilize the overall adaptive control over a long time period of operation.

The control signal is generated in a similar manner to those previously described:

$$\boldsymbol{u}(t) = \boldsymbol{K}_P(t)\boldsymbol{x}_{PE}(t) + \boldsymbol{K}_F(t)\boldsymbol{x}_{FE}(t) \tag{9}$$

where $\boldsymbol{K}_P(t)$, $\boldsymbol{K}_F(t) \in \Re^{m\times mn}$ are the adaptive gain matrices. Note that in the standard Er-MCSI algorithm, the vector $\boldsymbol{x}_I(t) = \boldsymbol{C}\int_0^t \boldsymbol{x}_{PE}(\tau)d\tau \in \Re^m$ is used instead of $\boldsymbol{x}_{FE}(t) \in \Re^{mn}$, with $\boldsymbol{C} = \mathrm{diag}\{\boldsymbol{c}, \boldsymbol{c}, \cdots, \boldsymbol{c}\} \in \Re^{mn\times m}$, $\boldsymbol{c} = \begin{bmatrix}1 \cdots 0\ 0\end{bmatrix}^T \in \Re^n$, and the $m\times m$ adaptive gain $\boldsymbol{K}_I(t)$ is used instead of $\boldsymbol{K}_F(t) \in \Re^{m\times mn}$. We generate a state error dynamic equation by using (5) and (6):

$$\begin{aligned}\dot{\boldsymbol{x}}_{PE}(t) &= \ddot{\boldsymbol{x}}(t) - \dot{\boldsymbol{x}}(t)\\ &= \bar{\boldsymbol{A}}\boldsymbol{x}_{PE}(t) - \boldsymbol{B}_E\boldsymbol{B}(t)\boldsymbol{K}_P(t)\boldsymbol{x}_{PE}(t) - \boldsymbol{B}_E\boldsymbol{B}(t)\boldsymbol{K}_F(t)\boldsymbol{x}_{FE}(t)\\ &\quad + (\bar{\boldsymbol{A}} - \boldsymbol{A}(t))\boldsymbol{x}(t) + \bar{\boldsymbol{B}}\boldsymbol{r}(t) - \boldsymbol{d}(t)\\ &= \bar{\boldsymbol{A}}\boldsymbol{x}_{PE}(t) - \boldsymbol{B}_E\boldsymbol{B}(t)\boldsymbol{K}_P(t)\boldsymbol{x}_{PE}(t) - \boldsymbol{B}_E\boldsymbol{B}(t)\boldsymbol{K}_F(t)\boldsymbol{x}_{FE}(t) + \boldsymbol{\xi}(t)\end{aligned} \tag{10}$$

where $\boldsymbol{\xi}(t) = (\bar{\boldsymbol{A}} - \boldsymbol{A}(t))\boldsymbol{x}(t) + \bar{\boldsymbol{B}}\boldsymbol{r}(t) - \boldsymbol{d}(t)$ can be rewritten, using (5) and (6), as:

$$\boldsymbol{\xi}(t) = -\bar{\boldsymbol{A}}\boldsymbol{x}_{PE} + \dot{\boldsymbol{x}}_{PE} + \boldsymbol{B}_E\boldsymbol{B}(t)\boldsymbol{u}(t) \tag{11}$$

Equation (10) suggests that $\boldsymbol{\xi}(t)$ is a vector that must be negated if the model following is perfectly achieved and we therefore treat $\boldsymbol{\xi}(t)$ as a disturbance vector.

Let us introduce the augmented error vector:

$$\boldsymbol{w}_E(t) \equiv \begin{bmatrix}\boldsymbol{x}_{PE}(t)^T & \boldsymbol{x}_{FE}(t)^T\end{bmatrix}^T \in \Re^{2mn}$$

and the augmented adaptive gain matrix,

$$\boldsymbol{\Phi}(t) \equiv \begin{bmatrix}\boldsymbol{B}(t)\boldsymbol{K}_P(t) & \boldsymbol{B}(t)\boldsymbol{K}_F(t)\end{bmatrix} \in \Re^{m\times 2mn}$$

Using $\boldsymbol{w}_E(t)$ and $\boldsymbol{\Phi}(t)$ in (10):

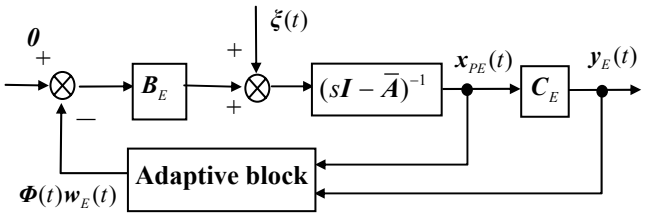

Fig.3 The closed error system with adaptive feedback

$$\dot{\boldsymbol{x}}_{PE}(t) = \bar{\boldsymbol{A}}\boldsymbol{x}_{PE}(t) - \boldsymbol{B}_E\boldsymbol{\Phi}(t)\boldsymbol{w}_E(t) + \boldsymbol{\xi}(t) \tag{12}$$

Also, define the output error vector:

$$\boldsymbol{y}_E(t) = \boldsymbol{C}_E\boldsymbol{x}_{PE}(t) \quad \in \Re^m \tag{13}$$

with the output error compensation matrix $\boldsymbol{C}_E \in \Re^{m\times mn}$. The closed-loop error dynamics described by (12) and (13) are illustrated in the block diagram as shown in Fig.3.

D. Design of a stable adaptive system

In order to stabilize the closed-loop error dynamics shown in Fig.1, two conditions must be satisfied. Firstly, in the linear forward loop, the compensator matrix $\boldsymbol{C}_E$ must be chosen so that the triple $\{\bar{\boldsymbol{A}}, \boldsymbol{B}_E, \boldsymbol{C}_E\}$ satisfies the strictly positive real (SPR) condition. Correspondingly, the Kalman-Yakubovich lemma states the positive definite symmetric matrix, $\boldsymbol{P}$, which solves the following Lyapunov equation:

$$\bar{\boldsymbol{A}}^T\boldsymbol{P} + \boldsymbol{P}\bar{\boldsymbol{A}} = -\boldsymbol{Q}, \quad \forall\boldsymbol{Q} > 0 \tag{14}$$

yields $\boldsymbol{C}_E$ according to:

$$\boldsymbol{C}_E = \boldsymbol{B}_E^T\boldsymbol{P} \tag{15}$$

thus satisfying the SPR condition [18], [21]. Since $\bar{\boldsymbol{A}}$ is designed to be positive definite, the matrix $\boldsymbol{P}$ is guaranteed to exist.

The second condition is that the adaptive block in the feedback loop must satisfy the passivity condition described by the following inequality [21]:

$$\int_0^t \boldsymbol{y}_E(\tau)^T\boldsymbol{\Phi}(\tau)\boldsymbol{w}_E(\tau)d\tau \geq \rho\int_0^t \boldsymbol{y}_E(\tau)^T\boldsymbol{y}_E(\tau)d\tau \tag{16}$$

for some positive scalar ρ. It follows from substituting $\boldsymbol{w}_E(t)$ and $\boldsymbol{\Phi}(t)$ into (16) that:

$$\begin{aligned}&\int_0^t \boldsymbol{y}_E^T(\tau)\boldsymbol{B}(\tau)\boldsymbol{K}_P(\tau)\boldsymbol{x}_{PE}(\tau)d\tau + \int_0^t \boldsymbol{y}_E^T(\tau)\boldsymbol{B}(\tau)\boldsymbol{K}_F(\tau)\boldsymbol{x}_{FE}(\tau)d\tau\\ &\qquad \geq \rho\int_0^t \boldsymbol{y}_E^T(\tau)\boldsymbol{y}_E(\tau)d\tau\end{aligned} \tag{17}$$

As a general choice of $\boldsymbol{K}_P(t)$ and $\boldsymbol{K}_F(t)$, we propose the following forms:

$$\begin{aligned}\boldsymbol{K}_P(t) &= G_P(q)\boldsymbol{y}_E(t)\boldsymbol{x}_{PE}^T(t) \quad \in \Re^{m\times mn}\\ \boldsymbol{K}_F(t) &= G_F(q)\boldsymbol{y}_E(t)\boldsymbol{x}_{FE}^T(t) \quad \in \Re^{m\times mn}\end{aligned} \tag{18}$$

where $G_P(q)$ and $G_F(q)$ are proper linear transfer functions, written in terms of the differential operator, q, which we call *adaptive gain filters*. Since $\boldsymbol{x}_{FE}(t) = \left(1/(q+\varepsilon_0)\right)\boldsymbol{x}_{PE}(t)$, (see (8)), $\boldsymbol{K}_F(t)$ can be written as:

$$\boldsymbol{K}_F(t) = \frac{1}{q+\varepsilon_0}G_F(q)\boldsymbol{y}_E(t)\boldsymbol{x}_{PE}^T(t) \quad \in \Re^{m\times mn} \tag{19}$$

Proposition
The passivity condition (17) is satisfied if the transfer functions $G_P(q)$ and $\left(1/(q+\varepsilon_0)\right)G_F(q)$ described in (18) and (19) are output strictly passive (OSP).

Proof
Let us consider the first term of the left hand side of (17):

$$f(t) = \int_0^t \boldsymbol{y}_E^T(\tau)\boldsymbol{B}(\tau)\boldsymbol{K}_P(\tau)\boldsymbol{x}_{PE}(\tau)d\tau$$

It follows from the substitution of (18) that:

$$f(t) = G_P(q)\int_0^t \boldsymbol{y}_E^T(\tau)\boldsymbol{B}(\tau)\boldsymbol{y}_E(\tau)\boldsymbol{x}_{PE}^T(\tau)\boldsymbol{x}_{PE}(\tau)d\tau$$

Since $\boldsymbol{B}(t)$ is symmetric, it can be factorized as $\boldsymbol{B}(t) = \sqrt{\boldsymbol{B}(t)}^T\sqrt{\boldsymbol{B}(t)}$. Substituting this into the above equation yields:

$$f(t) = G_P(q)\int_0^t \left(\sqrt{\boldsymbol{B}(\tau)}\boldsymbol{y}_E(\tau)\right)^T\left(\sqrt{\boldsymbol{B}(\tau)}\boldsymbol{y}_E(\tau)\right)\boldsymbol{x}_{PE}^T(\tau)\boldsymbol{x}_{PE}(\tau)d\tau$$

Since $G_P(q)$ is output strictly passive (OSP), we can always find ρ_1 such that:

$$f(t) \ge \rho_1^2\left|G_P(i\omega)\right|^2\int_0^t \left(\sqrt{\boldsymbol{B}(\tau)}\boldsymbol{y}_E(\tau)\right)^T\left(\sqrt{\boldsymbol{B}(\tau)}\boldsymbol{y}_E(\tau)\right)\boldsymbol{x}_{PE}^T(\tau)\boldsymbol{x}_{PE}(\tau)d\tau$$

for all ω. Since $\sqrt{\boldsymbol{B}(t)}$ is bounded and strictly positive definite, we can also find ρ_2 such that $\left|\sqrt{\boldsymbol{B}(t)}\right| > \rho_2$. Therefore, since $\boldsymbol{x}_{PE}(t)$ is linearly related to $\boldsymbol{y}_E(t)$ by (13) we can always find ρ_3 such that:

$$\int_0^t \boldsymbol{x}_{PE}^T(\tau)\boldsymbol{x}_{PE}(\tau)d\tau \ge \rho_3^2\int_0^t \boldsymbol{y}_E^T(\tau)\boldsymbol{y}_E(\tau)d\tau$$

Consequently it follows that:

$$f(t) \ge \rho_1^2\rho_2^2\rho_3^2\left|G_P(i\omega)\right|^2\int_0^t \boldsymbol{y}_E^T(\tau)\boldsymbol{y}_E(\tau)d\tau$$

A similar result applies to the second term of the left hand side of (17), hence the proposition is proven to be valid. □

Remark 1. $G_P(q)$ or $\left(1/(q+\varepsilon)\right)G_F(q)$ must be OSP and should not be simply SPR, or input strictly passive (ISP). The SPR and the ISP conditions only require $\mathrm{Re}[G(i\omega)] > 0$ for a transfer function that is analytic in the right half plane. But we must ensure that $\left|G(i\omega)\right|$ is bounded for all ω. Note that the 'PI' adaptation laws [18], that the MRAC and MCS have used to date, are not OSP, although they are SPR, since the corresponding transfer functions are of the form $\beta + \alpha/s,\ (\alpha, \beta > 0)$.

Remark 2. The OSP condition on $G_F(q)$ is stricter than that on $G_P(q)$, since $\left(1/(q+\varepsilon)\right)G_F(q)$ already has nearly $-\pi/2$ of phase shift across most of the frequency spectrum, due to the term $1/(q+\varepsilon)$ and the small value of ε. Hence $G_F(q)$ must have a phase margin less than $\pi/2$ and greater than 0.

IV. Simulation Study

This section describes a simulation study of the new method (known as the generalized Er-MCSI algorithm) applied to the control of a serial link manipulator. Such a system is typical of a non-linear coupled mechanical system.

A. Plant description

The mechanical model for the simulation is a two link serial manipulator, as shown in Fig.3. The gravitational acceleration works downward (in the opposite direction to the *y*-axis) and the physical parameters are chosen as follows:

$$l_1 = 0.3m,\ l_1 = 0.2m,\ r_1 = r_2 = 0.1m,$$
$$m_1 = 3kg,\ m_2 = 2kg,\ m_3 = 1kg,\ J_1 = 0.03kgm^2, J_2 = 0.02kgm^2$$

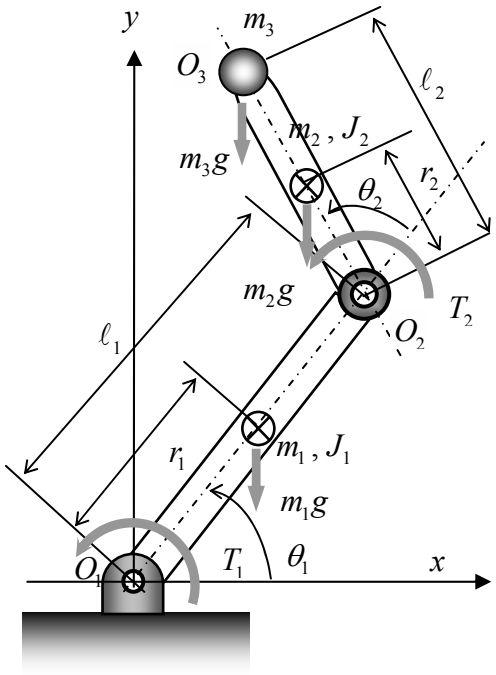

Fig.4 Configuration of a two serial link manipulator

The initial conditions on the link angles are $\theta_1 = \theta_2 = 0$, which means the arm starts from a horizontal posture and therefore suffers from the worst possible case of maximum gravitational moment force at $t = 0$. In addition, the actuator input torque limitations are assumed to be $-u_{Li} \le u_i \le u_{Li}$, $(i = 1, 2)$.

B. Decoupled linear reference model

The linear reference model is a two-DOF decoupled second-order model. According to (6) we therefore have:

$$\bar{\boldsymbol{x}}(t) = \begin{bmatrix} \bar{\theta}_1 & \dot{\bar{\theta}}_1 & \bar{\theta}_2 & \dot{\bar{\theta}}_2 \end{bmatrix}^T$$

$$\bar{\boldsymbol{A}} = \begin{bmatrix} 0 & 1 & 0 & 0 \\ -\omega_{n1}^2 & -2\zeta_1\omega_{n1} & 0 & 0 \\ 0 & 0 & 0 & 1 \\ 0 & 0 & -\omega_{n2}^2 & -2\zeta_2\omega_{n2} \end{bmatrix},\quad \bar{\boldsymbol{B}} = \begin{bmatrix} 0 & 0 \\ \omega_{n1}^2 & 0 \\ 0 & 0 \\ 0 & \omega_{n2}^2 \end{bmatrix}$$

with the natural frequencies ω_{n1}, ω_{n2} and the damping ratios ζ_1, ζ_2. These are determined as:

$\omega_{n1} = \omega_{n2} \simeq 4/t_s$, $\zeta_1 = \zeta_2 = 1$, for a given settling-time, t_s.

C. Synthesis of the compensator matrix, $\boldsymbol{C}_E$

The compensator matrix $\boldsymbol{C}_E$ has to be determined in order to satisfy the Kalman-Yakubovich lemma, (14) and (15), when:

$$\bar{\boldsymbol{A}} = \begin{bmatrix} 0 & 1 & 0 & 0 \\ -\omega_{n1}^2 & -2\zeta_1\omega_{n1} & 0 & 0 \\ 0 & 0 & 0 & 1 \\ 0 & 0 & -\omega_{n2}^2 & -2\zeta_2\omega_{n2} \end{bmatrix}, \quad \boldsymbol{B}_E = \begin{bmatrix} 0 & 0 \\ 1 & 0 \\ 0 & 0 \\ 0 & 1 \end{bmatrix}$$

As a candidate of the positive definite symmetric matrix $\boldsymbol{P}$ we choose:

$$\boldsymbol{P} = \begin{bmatrix} d_1/\zeta_1 + 2\zeta_1 & 1/\omega_{n1} & 0 & 0 \\ 1/\omega_{n1} & d_1/\left(\zeta_1\omega_{n1}^2\right) & 0 & 0 \\ 0 & 0 & d_2/\zeta_2 + 2\zeta_2 & 1/\omega_{n2} \\ 0 & 0 & 1/\omega_{n2} & d_2/\left(\zeta_2\omega_{n2}^2\right) \end{bmatrix}$$

where d_1 and d_2 are non-dimensional free parameters. The matrix $\boldsymbol{Q}$ is then obtained, according to (14), as:

$$\boldsymbol{Q} = 2\begin{bmatrix} \omega_{n1} & 0 & 0 & 0 \\ 0 & \left(2d_1 - 1\right)/\omega_{n1} & 0 & 0 \\ 0 & 0 & \omega_{n2} & 0 \\ 0 & 0 & 0 & \left(2d_2 - 1\right)/\omega_{n2} \end{bmatrix}$$

In order to assure the positive definiteness of $\boldsymbol{Q}$ we set:

$$d_i > 0.5 \quad (i = 1, 2)$$

so that the corresponding $\boldsymbol{C}_e$ is obtained via (15) as:

$$\boldsymbol{C}_e = \begin{bmatrix} 1/\omega_{n1} & d_1/(\zeta_1\omega_{n1}^2) & 0 & 0 \\ 0 & 0 & 1/\omega_{n2} & d_2/(\zeta_2\omega_{n2}^2) \end{bmatrix} \quad (20)$$

Note that the rôle of the compensator matrix $\boldsymbol{C}_e$ is identical to the construction of a 'sliding surface' as described in [2], [6]-[8]. In particular, (13) with (20) yields:

$$\begin{bmatrix} y_{E1} \\ y_{E2} \end{bmatrix} = \begin{bmatrix} (1/\omega_{n1})x_{PE1} + \left(d_1/(\zeta_1\omega_{n1}^2)\right)\dot{x}_{PE1} \\ (1/\omega_{n2})x_{PE2} + \left(d_2/(\zeta_2\omega_{n2}^2)\right)\dot{x}_{PE2} \end{bmatrix}$$

which are none other than sliding surfaces. In the simulations we set $d_1 = d_2 = 1$, which provide stable tracking performances.

D. Adaptive gain filter parameters

Two types of adaptive gain filters were tested:

Type 1: $$G_P(q) = G_F(q) = \beta + \alpha/(q + \varepsilon) \quad (21)$$

Type 2: $$\left\{\begin{matrix} G_P(q) = \beta/(\gamma^2 q^2 + \tau\gamma q + 1) \\ G_F(q) = \beta + \alpha/(q + \varepsilon) \end{matrix}\right\} \quad (22)$$

Those choices satisfy the OSP condition on $G_P(q)$ and $\left(1/(q+\varepsilon)\right)G_F(q)$. The type 1 filter is almost the same as the normal MRAC/MCS approach ($G_P(q) = G_F(q) = \beta + \alpha/q$), except that the pure integration term is replaced by a first-order filter in order to satisfy the OSP condition. Usually, the parameter ε is assigned to a small value (the same value as ε_0 in (19)), so that the type 1 filter may be considered to be a virtual PI filter with proportional gain β and integral gain α. In the type 2 filter, $G_P(q)$ is of second-order with a natural frequency $1/\gamma$ and damping ratio $\tau/2$.

E. Simulation results

A square-wave signal of 2s period, 0.5rad amplitude and an offset of 0.5rad is used as the reference signal for both links, but with a $\pi/2$rad phase shift between them, in order to examine any cross-coupling effects in the responses. The settling-time t_s of the linear model is assigned to be 0.3s for most of the simulations. A set of four simulation studies are described below.

(1) Normal input torque limits are applied: 30Nm for link 1 motor and 11Nm for link 2 motor

Fig.5 shows the step response of the PID controller, and the proposed type 1 and 2 Er-MCSI controllers under the normal torque limits: 30Nm for the motor drive on link 1 and 11Nm on link 2. These values are reasonable, since approximately 16Nm and 4Nm, respectively, are required to sustain the initial horizontal posture of the manipulator. As shown in Fig.5, all of the controllers yield a similar performance, with no discernable coupling effects between the links. Note that the tuning of the PID controller requires the determination of 6 gains (3 for each link) – a not inconsiderable effort.

(2) Strictly limited input torque limits are applied: 20Nm for link 1 motor and 7.3Nm for link 2 motor

Fig.6 shows the results of repeating the simulation of Fig.5, except the input torques are strictly limited to 20Nm for motor 1 and 7.3Nm for motor 2. These values are only slightly larger than those required to sustain the initial horizontal posture. For the PID controller, the P, I and D-gains are appropriately re-tuned. It is observed that θ_1 sinks below the 0 reference line, when using the type 1 Er-MCSI controller; (Fig.6 (b)). This is due to the gravitational moment being nearly of the same value as the maximum available motor torque. However, the type 2 Er-MCSI controller almost succeeds in preventing this phenomenon, as a result of increasing the parameter γ; (Fig.6 (c)). In this case, an initial sinking effect is observed only during the early stages of adaption.

We observe that there is another method of coping with the severe limitations of the input torque when using the type 1 and 2 Er-MCSI controllers. That is, to increase the settling-time, t_s, of the linear reference model. Thus, in Fig.7 the settling-time is increased to 0.35s, from the 0.3s used in Figs.5 and 6. As a result, the type 1 and 2 Er-MCSI controllers show a much improved performance that is now superior to that of the PID controller in Fig.6 (a).

(3) Control with observation noise.

To investigate the sensitivity of the controllers under the influence of observation noise, we simulate the effect of the angular velocity measurement being contaminated with band-limited white noise, of maximum amplitude ~ 2rad/s. In

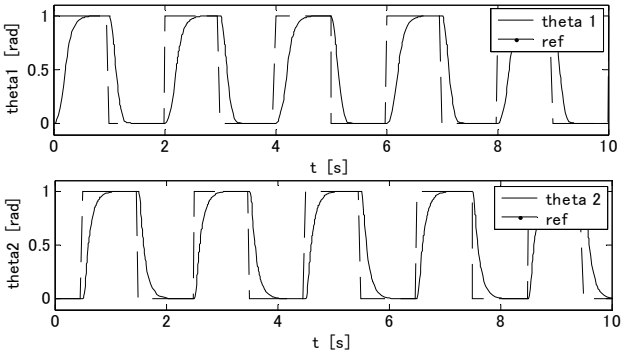

(a) Best tuned PID controller

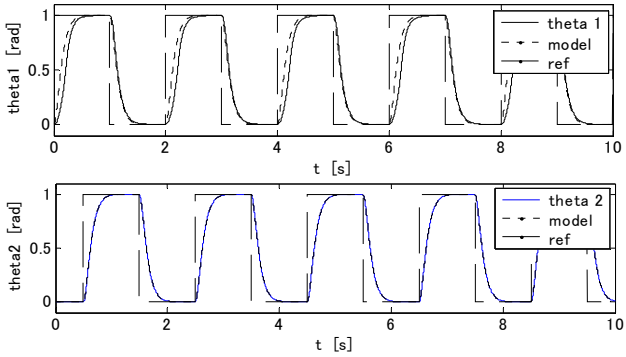

(b) Type 1 Er-MCSI controller

($\alpha = 10^7$, $\beta = 10^9$, $\varepsilon = 0.1$)

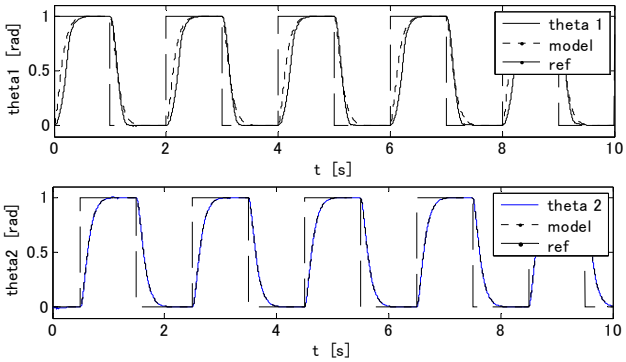

(c) Type 2 Er-MCSI controller

($\alpha = 10^7$, $\beta = 10^9$, $\varepsilon = 0.1$, $\gamma = 0.01$, $\tau = \sqrt{2}$)

Fig.5 Step responses of the PID controller and the type 1 and the type 2 Er-MCSI controllers under normal input torque limits

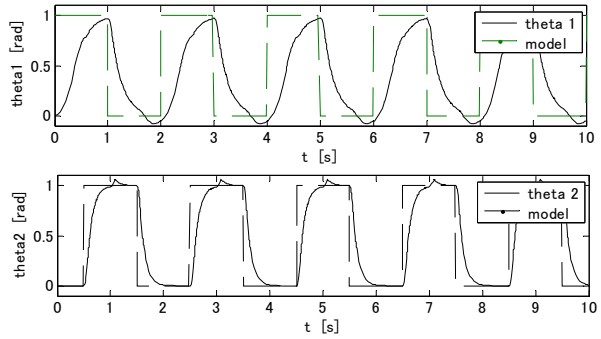

(a) Best tuned PID controller

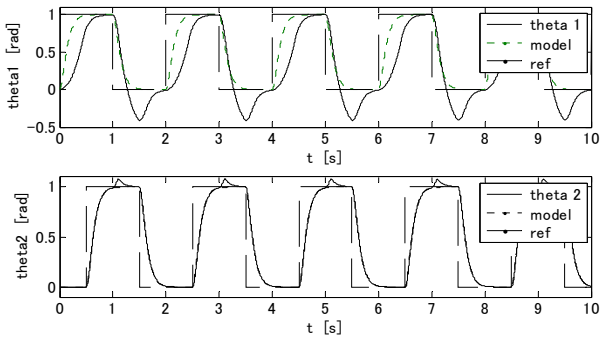

(b) Type 1 Er-MCSI controller

($\alpha = 10^7$, $\beta = 10^9$, $\varepsilon = 0.1$)

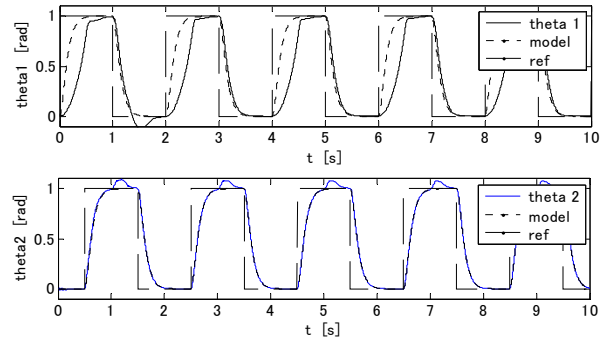

(c) Type 2 Er-MCSI controller

($\alpha = 10^7$, $\beta = 10^9$, $\varepsilon = 0.1$, $\gamma = 0.04$, $\tau = \sqrt{2}$)

Fig.6 Step responses of the PID controller and the proposed type 1 and the type 2 Er-MCSI controllers under strictly limited input torque.

order to emphasise the resulting effects, the noise amplitude is somewhat exaggerated with respect to the maximum amplitudes of link velocity, which are ~ 5rad/s.

Fig.8 shows the performance of the types 1 and 2 Er-MCSI controllers. Again we observe the initial sinking phenomenon of θ_1 with the type 2 controller, then a gradual recovery as time progresses. Overall, both of the controllers are satisfactory in their insensitivity to the large amplitude observation noise.

(4) Wind-up suppression of the adaptive gains

We now employ first-order filters in the process of generating the adaptive gains (see (19), (21) and (22)) to suppress potential wind-up, [20]. To see the effect, we observe the adaptive gains over a relatively long simulation time, as shown in Fig.9. Only the elements of the adaptive gain matrix $\boldsymbol{K}_F$ are shown, since the elements of $\boldsymbol{K}_E$ do not show the wind-up effect.

There are eight entries in the matrix $\boldsymbol{K}_F$, but only a few of the larger amplitude entries can be clearly distinguished in the figures. When ε_0 and ε are both set to zero, wind-up is exhibited by both the type 1 and 2 Er-MCSI controllers (Figs 9(a) and 9(c)). This wind-up of the adaptive gains is due to

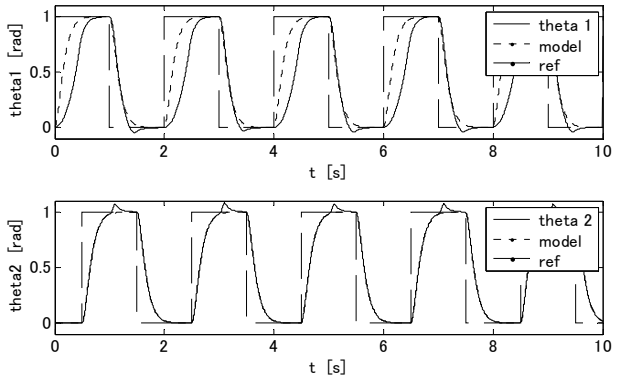

(a) Type 1 Er-MCSI controller
($\alpha = 10^7, \beta = 10^9, \varepsilon = 0.1$)

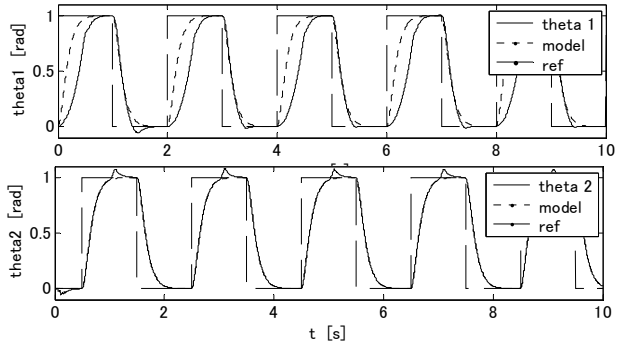

(b) Type 2 Er-MCSI controller
($\alpha = 10^7, \beta = 10^9, \varepsilon = 0.1, \gamma = 0.01, \tau = \sqrt{2}$)

Fig.7 Step responses of the proposed type 1 and the type 2 controllers under strictly limited input torque. The settling time $t_s = 0.35s$

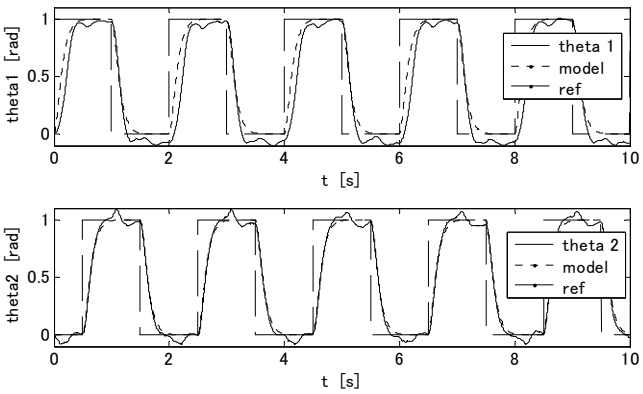

(a) Type 1 Er-MCSI controller
($\alpha = 10^7, \beta = 10^9, \varepsilon = 0.1$)

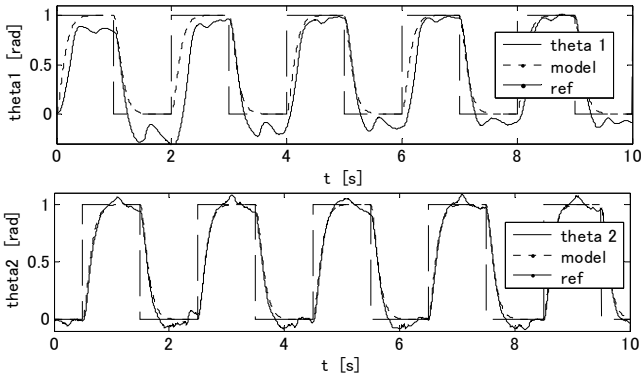

(b) Type 2 Er-MCSI controller
($\alpha = 10^7, \beta = 10^9, \varepsilon = 0.1, \gamma = 0.01, \tau = \sqrt{2}$)

Fig.8 Step responses of the type 1 and type 2 Er-MCSI controllers with observation noise on the angular velocity measurement.

the input torque limitation and the observation noise, both of which provide model-following errors. If left to continue, wind-up of the adaptive gains will degenerate the model-following performance and possibly lead to instability.

However, as seen in Figs 9(b) and 9(d), the first-order filter of (19), (21) and (22) effectively suppresses the wind-up.

(5) Tuning the parameters of type 1 and 2 Er-MCSI controllers

All of the parameters used in the type 1 and 2 Er-MCSI controllers can admit a wide range of tuning. Every parameter, except γ, is dimensionless, so that each one can be selected as a constant value, irrespective to the plant size. Only the parameter γ has the dimension of time, so it should be determined according to the required settling-time, t_s. Our observations suggest that γ should be less than one-tenth the value of t_s. However, an excessively small value of γ increases noise sensitivity. The adaptive weights α and β are tuneable in a four or five decade range, and from the simulations in this paper, our observations suggest that good performance can be obtained when α is approximately one-hundredth the value of β.

The parameters d and τ have a similar effect to damping coefficients and should be determined within the range 0.5-2.0. The parameters ε_0 and ε have identical rôles - their reciprocal values specify the DC-gain of the integrators. We specify a value of 0.1 for both of them, ensuring that the adaptive gains settle within ~ 20s.

V. CONCLUSIONS

In this paper we have proposed a generalized and improved error-based minimum control synthesis algorithm with integral action (Er-MCSI). This adaptive controller can improve on the performance characteristics of MRAC [18], MCS [14]-[17] and basic Er-MCSI [19]. In common with MCS, the new controller does not require any *a priori* parametric knowledge of the controlled plant. In common with Er-MCSI, the new algorithm is also insensitive to the operating points of the plant and the reference model.

Stability analysis was performed for the new generalized algorithm using passivity concepts.

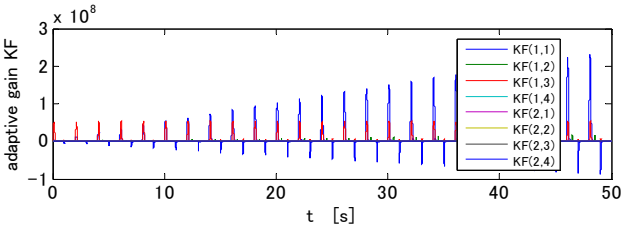

(a) Adaptive gains K_F of the type 1 Er-MCSI controller $\varepsilon_0 = \varepsilon = 0$

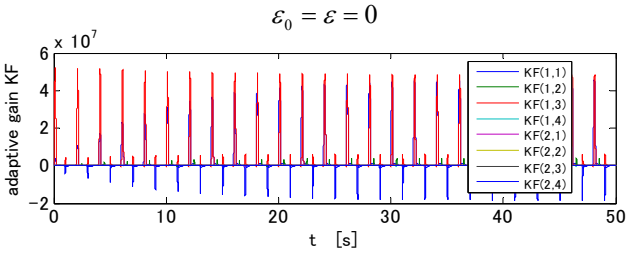

(b) Adaptive gains K_F of the type 1 Er-MCSI controller $\varepsilon_0 = \varepsilon = 0.1$

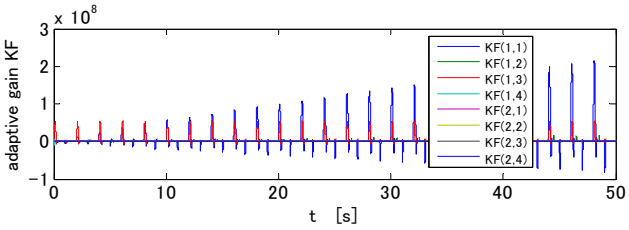

(c) Adaptive gains K_F of the type 2 Er-MCSI controller $\varepsilon_0 = \varepsilon = 0$

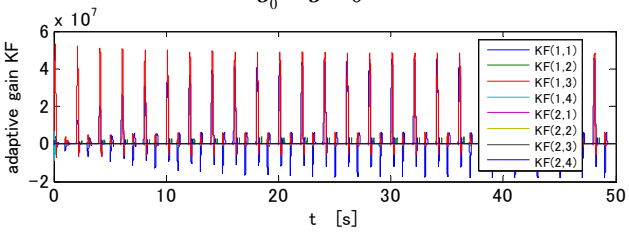

(d) Adaptive gains K_F of the type 2 Er-MCSI controller $\varepsilon_0 = \varepsilon = 0.1$

Fig.9 Adaptive gain K_F of the type 1 and 2 Er-MCSI controllers during extended simulation time.

Simulation studies upon a two-link manipulator, with non-linear, coupled dynamics, are also described. In the simulations we proposed two types of the new controller, that both satisfy the stability condition. The detailed design procedures for these controllers were also described.

The simulation studies demonstrated excellent model-following performance under some severe test conditions: significant gravitational moments, restrictive actuator torque limitations and large levels of observation noise contamination. We also demonstrated that the proposed method for suppressing adaptive gain wind-up was successful.

ACKNOWLEDGEMENTS

The authors gratefully acknowledge the support of Tokai University, Kanagawa Prefecture and the Royal Society of London (Grant JP/16371) in the pursuance of this work.

REFERENCES

[1] J. J. Craig, P. Hsu and S. S. Sastry, "Adaptive Control of Mechanical Manipulators," Proc. of IEEE International Conference on Robotics and Automation, 1986, pp.190-195.

[2] J.-J. E. Slotine and W. Li, "On the Adaptive Control of Robot Manipulators," The International Journal of Robotics Research, Vol.6, No.3, 1987, pp.49-59.

[3] N. Sadegh and R. Horowitz, "Stability and Robustness Analysis of a Class of Adaptive Controller for Robotic Manipulators," The International Journal of Robotics Research, Vol.9, No.3, 1990, pp.74-92.

[4] M. W. Spong and R. Ortega, "On Adaptive Inverse Dynamics Control of Rigid Robots," IEEE Trans.on Automatic Control, Vol.35, No.1, 1990, pp.92-95.

[5] P. Tomei, "Adaptive PD Controller for Robot Manipulators," IEEE Trans.on Robotics and Automation, Vol.7, No.4, 1991, pp.565-570.

[6] Y. Tang and M. A. Arteaga, "Adaptive Control of Robot Manipulators Based on Passivity," IEEE Trans.on Automatic Control, Vol.39, No.9, 1994, pp.1871-1875.

[7] L. Villani, C. C. de Wit and B. Brogliato, "An Exponentially Stable Adaptive Control for Force and Position Tracking of Robot Manipulators," IEEE Trans. on Automatic Control, Vol.44, No.4, 1999, pp.798-802.

[8] Y.-H. Liu, K. Kitagaki, T. Ogasawara and S. Arimoto, "Model-Based Adaptive Hybrid Control for Manipulators Under Multiple Geometric Constraints," IEEE Trans. on Control System Technology, Vol.7, No.1, 1999, pp.97-109.

[9] A. Laib, "Adaptive Output Regulation of Robot Manipulator Under Actuation Constraints," IEEE Trans. on Robotics and Automation, Vol.16, No.1, 2000, pp.29-35.

[10] S. R. Bowes and J. Li, "New Robust Adaptive Control Algorithm for High Performance AC Drives," IEEE Trans. on Industrial Electronics, Vol.47, No.2, 2000, pp.325/336.

[11] K. C. Jin, H. W. Yong and L. C. Goo, "Speed Control of PMSM Using a Robust Adaptive Controller," Proc. of the 40th SICE Annual Conference, 2001, 112A-4, pp.12-15.

[12] B. Catino, S. Santini and M. di Bernardo, "MCS Adaptive Control of Vehicle Dynamics: an Application of Bifurcation Techniques to Control System Design," Proc. of the 42nd IEEE Conference on Decision and Control, Maui, Hawaii USA, 2003, WeM08-2, pp.2252-2257.

[13] T. T. Arif, "A Modified Minimal Controller Synthesis for Satellite Attitude Control," Proc. of Aerospace Conference, 2006, IEEE, pp.1-7.

[14] D. P. Stoten and H. Benchoubane, "Robustness of a Minimal Controller Synthesis Algorithm," International Journal of Control, Vol.51, No.4, 1990, pp.851-861.

[15] D. P. Stoten and H. Benchoubane, "The Extended Minimal Controller Synthesis Algorithm," International Journal of Control, Vol.56, No.5, 1992, pp.1139-1165.

[16] S. P. Hodgson and D. P. Stoten, "Passivity-based Analysis of the Minimal Control Synthesis Algorithm," International Journal of Control, Vol.63, No.1, 1996, pp.67-84.

[17] S. P. Hodgson and D. P. Stoten, "Robustness of the Minimal Control Synthesis Algorithm to Non-linear Plant with Regard to the Position Control of Manipulator," International Journal of Control, Vol.72, No.14, 1999, pp.1288-1298.

[18] Y. D. Landau, *Adaptive Control: The Model Reference Approach*, Marcel Dekker Inc., 1979.

[19] D. P. Stoten and S. A. Neild, "The error-based minimal control synthesis algorithm with integral action," Proc of Instn. Mech. Engrs. Vol.217, Part I: J. System and Control Engineering, 2003, pp.187-201.

[20] W.Niu and M. Tomizuka, "An Anti-Windup Design for Linear System with Asymptotic Tracking Subjected to Actuator Saturation," ASME Journal of Dynamic Systems, Measurement and Control, Vol.122, 2000, pp.369-374.

[21] K. J. Astrom and B. Wittenmark, *Adaptive Control,* 2nd Ed. Addison-Wesley, 1995.